A Practical Methodology for Fault Location in Transmission Lines Without Line Parameter Settings and Data Synchronization

Penta Rithisha[1], O. D. Naidu[1], Vedanta Pradhan[1] and Nandiraju Venkata Srikanth[2]*

[1]*Grid Automation R&D, Hitachi Energy, Bangalore, India*
[2]*Department of Electrical Engineering, National Institute of Technology, Warangal, India*
**od.naidu@hitachienergy.com*

Keywords: FAULT LOCATION, DATA SYNCHRONIZATION, LINE PARAMETER, TRANSMISSION LINE, PROTECTIVE RELAY

Abstract

Reliable fault location for power transmission networks requires line parameters and time synchronized voltage and current measurements from all terminals which may not always be available. In this work, a setting-free fault location methodology using unsynchronized data from the line terminals is proposed. This requires computation of data synchronization error which manifests as a phase angle error between the two terminal phasor measurements. The data synchronization angle is computed using unsynchronized phasors and a design factor related to the line. The design factor can be estimated from a set of synchronized measurements and stored. Upon detecting failure of the data synchronization mechanism, the same can be used to calculate the data synchronization angle between the unsynchronized measurements. The line parameters and subsequently fault location is computed using unsynchronized data and the estimated data synchronization angle. The proposed solution is verified using laboratory experimental and field data and it is found to be accurate.

1 Introduction

Transmission lines frequently encounter both temporary and permanent faults as a result of mechanical or environmental conditions, such as trees falling on the lines, lightning strikes, insulator degradation, etc. It is quite challenging for the substation maintenance crew to manually identify the location of a permanent fault on a transmission line, and this operation takes a lot of time and cost [1, 2]. This will ultimately cause the line to be down for a longer period, which is undesirable. Therefore, there is a need for reliable and accurate fault location technology that can aid in reducing the amount of human work required to locate the fault.

Since decades, there are many existing fault location methods in the literature. Depending on the availability of the input signals, fault location methods can be classified into single ended [3]-[5] and double ended [9]-[21]. Single ended impedance-based methods [3, 4] are simple and easy to implement in relays as it does not require communication and data synchronization. However, the accuracy of these methods depends on fault loop information, local and remote source impedance values and system non-homogeneity, mutual compensation etc. [5]. Moreover, these methods may not provide accurate location for lines connected with inverter-based resources due to introduction of high non-homogeneity [6]-[8]. Therefore, these methods may not be reliable and accurate for modern power grids with renewable integration.

Traveling wave-based fault locators are a promising technique due to recent advancements in data gathering and signal processing [9]. This technique makes it feasible to locate faults with greater accuracy at a distance of two tower spans (~300 m). Traveling wave based single ended [10], double ended [9], setting-free [11], unsynchronized data [12] are proposed. Practical implementation of the single ended traveling wave-based methods is difficult as it requires identification of the origin of the second reflection (i.e., reflected from the fault point or remote bus or any other impedance discontinuity position). Though the communication based double ended methods are accurate, they require the hardware with a higher sampling rate (MHz) and a large communication bandwidth. Additionally, the practical application of this technology necessitates the fine-tuning of numerous parameters, which raises the engineering and total cost of the solution [20].

Present communication technology allows for use of data from both ends of the line to calculate the location of the fault [13]. The accuracy of double-ended methods is not affected by fault resistance, loading, fault loop information, and system non-homogeneity. These methods are economical alternative to traveling wave-based methods that requires high sampling rates. Communication based fault location methods using synchronized [13] and unsynchronized data [14]-[17] are presented. However, the precision of these methods depends on accuracy of their line parameter settings [18]. The electrical parameters of a transmission line are not known with great precision. It is noted in case studies that there is up to 25-30% of error in actual and the stored values of the line parameters [19]. Fault location algorithms are sensitive to line parameters. Small error in line parameters can lead to high error in fault location estimation.

Recently, a setting-free method to locate the fault in transmission line is presented in [20] using synchronized data. This method calculates the required line parameters using pre-fault data and determine the location of the fault using the estimated parameters and during fault phasors from both ends of the line. Though this method is accurate, its performance is

https://doi.org/10.1049/icp.2024.0896

subject to data synchronization. A promising method to locate the fault in transmission lines without parameter settings and data synchronization is presented in [21]. This method estimates the synchronization angle and parameters using the pre-fault unsynchronized voltage and current measurements at both ends of the line. The fault location is calculated using the estimated parameters, synchronization angle and unsynchronized voltage and current phasors during fault. However, this method does not provide reliable estimates of data synchronization angle for loading conditions due to underlying assumptions on line parameter. This leads to inaccurate fault location. A detailed mathematical analysis and limitations of this paper is discussed in the next section. Therefore, there is scope for improvement in fault location without using parameter settings and data synchronization. In this work, one such methodology is proposed. The key highlight of this method is the inclusion of a design factor related to the line which avoids corruption of the synchronization angle estimation due to line loading. This subsequently ensures high accuracy in fault location estimate. The proposed solution is verified using laboratory experimental and field data and it is found to be accurate.

2. Detailed Analysis of Synchronization Angle

In this section, a detailed mathematical analysis is provided for the data synchronization angle. The analysis provided in [21] is extended here to understand the limitations in the method proposed thereof for calculating the synchronization angle. Fig.1(a) is a schematic of two-terminal transmission line. Fig.1(b) and (c) represent the long line π equivalent positive sequence distributed line model during pre-fault and during-fault.

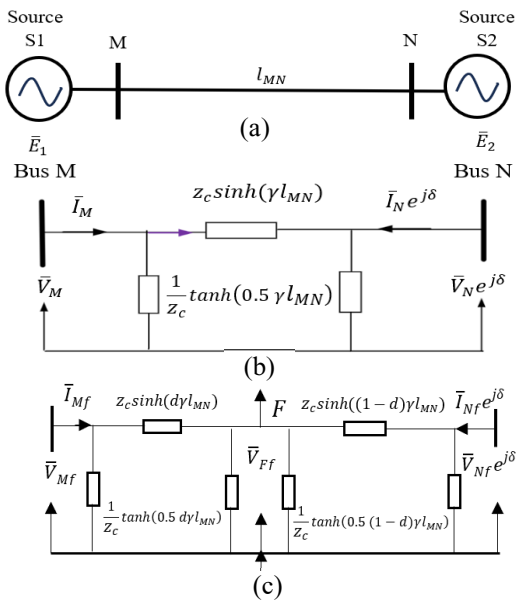

Fig.1. (a) Single line diagram, (b) pre-fault equivalent network and (c) during fault equivalent network.

$\bar{V}_M$, $\bar{V}_N$, $\bar{I}_M$, $\bar{I}_N$ are positive sequence voltages and currents of both ends as shown in the figure. Symbol l_{MN} denotes the length of the line, γ and z_c are positive sequence propagation constant and surge impedance of the line respectively. The data synchronization mismatch between the two terminals M and N is represented using a synchronization operator $e^{j\delta}$ where δ is the synchronization angle. From Fig. 1(a), the distributed line equations can be given as below:

$$\bar{V}_N e^{j\delta} = \bar{V}_M \cosh \gamma l_{MN} - \bar{I}_M z_c \sinh \gamma l_{MN} \quad (1)$$

$$\bar{I}_N e^{j\delta} = = \frac{1}{z_c} \bar{V}_M \sinh \gamma l_{MN} - \bar{I}_M \cosh \gamma l_{MN} \quad (2)$$

By eliminating z_c using (1) and (2), we can obtain (3)

$$\cosh \gamma l_{MN} = \bar{F}_1 e^{j\delta} + \frac{\bar{F}_2}{e^{j\delta}} \quad (3)$$

where,

$$\bar{F}_1 = \frac{\bar{V}_N \bar{I}_N}{(\bar{V}_M \bar{I}_N - \bar{V}_N \bar{I}_M)} \quad ; \; F_2 = \frac{-\bar{V}_M \bar{I}_M}{(\bar{V}_M \bar{I}_N - \bar{V}_N \bar{I}_M)}$$

Let the propagation constant $\gamma = \alpha + j\,\beta$. In the method presented in [21], it is assumed for EHV lines $\beta \gg \alpha$ which leads to the equation below:

$$\cosh \gamma l_{MN} - (\cosh \gamma l_{MN})^* = 0 \quad (4)$$

By substituting (3) in (4), the equation for the estimated synchronization angle obtained in [21] is as follows:

$$e^{j\delta_{est}} = \sqrt{\left(\frac{\bar{F}_2 - \bar{F}_1^*}{\bar{F}_2^* - \bar{F}_1}\right)} \quad (5)$$

Thus, the method of [21] provides a closed form solution for calculating the synchronization angle (i.e., the expression in (5)). Using this estimate of the synchronization angle, first the line parameters can be calculated using pre-fault unsynchronized voltages and currents of both the ends. Then these parameter estimates are used to calculate the fault location using the unsynchronized voltages and currents measured during fault. These formulations shall be presented later in this paper as well. It is important to note that estimates of the line parameters and subsequently the fault location are subject to the accuracy of the estimate of the data synchronization angle. It will now be shown that the assumption made in deriving the expression (5) can lead to significant errors in the estimation of the synchronization angle. The nature of the errors introduced in relation to the line loading shall also be discussed based on a mathematical analysis of the expression (5). The same shall also be illustrated with case studies of synchronized and unsynchronized measurements under different loading conditions of a two-terminal transmission line. Using properties of complex numbers on (5), we have

$$e^{j2\delta_{est}} = \frac{(\bar{F}_1^* - \bar{F}_2)}{(\bar{F}_1 - F_2^*)} = \frac{(\bar{F}_1^* - \bar{F}_2) \times (\bar{F}_1^* - \bar{F}_2)}{|(\bar{F}_1^* - \bar{F}_2)|^2} \quad (6)$$

From (6), a relation can be obtained as follows,

$$2\delta_{est} = 2 \arg(\bar{F}_1^* - \bar{F}_2) \quad (7)$$

From (7), it can be inferred that, the expression (5) provides the argument of $(\bar{F}_1^* - \bar{F}_2)$ as the estimated synchronization angle. $\bar{F}_1, \bar{F}_2$ are dependent on positive sequence voltages and currents of both ends as given as defined earlier in (3). Considering $(\bar{V}_M \bar{I}_N - \bar{V}_N \bar{I}_M) = \Delta$, it can be shown that

$$\bar{F}_1^* - \bar{F}_2 = \frac{\bar{V}_N^* \bar{V}_M (|\bar{I}_N|^2 - |\bar{I}_M|^2)}{|\Delta|^2} - \frac{\bar{I}_N^* \bar{I}_M (|\bar{V}_N|^2 - |\bar{V}_M|^2)}{|\Delta|^2} \quad (8)$$

Let us denote terms on the RHS of (8) as K_V and K_I, i.e.,

$$K_V = \frac{\bar{V}_N{}^* \bar{V}_M(|I_N|^2 - |I_M|^2)}{|\Delta|^2} \text{ and } K_I = \frac{I_N{}^* I_M(|\bar{V}_N|^2 - |\bar{V}_M|^2)}{|\Delta|^2}$$

Under light loading condition of the line when $|\bar{V}_N| \approx |\bar{V}_M|$, and the currents are small in magnitude, the argument of $(\bar{F}_1^*\text{-}\,\bar{F}_2)$ is primarily determined by that of K_V. This implies the phase angle obtained from (5) will correspond to the overall phase angle separation between the two end voltages, i.e., $\delta_{est} = \delta + \psi$, where ψ (in this case) is the line loading angle and δ is the data synchronization angle between the two terminals. At higher loading of the line, when $|\bar{V}_N| \approx |\bar{V}_M|$ may not be satisfied, and line current magnitudes are high, argument of $(\bar{F}_1^*\text{-}\,\bar{F}_2)$ is determined by both K_V and K_I and the angle ψ may not solely represent the line loading angle. In summary, the angle obtained by (5) generally is not only the synchronization angle. It is corrupted by an extra value which depends on the line loading. The only scenario in which the angle δ_{est} obtained using (5) indicates the synchronization angle δ is near no-load condition, i.e., when ψ is close to zero.

We now illustrate the above analyses by the help of a two terminal 400 kV, 50 Hz test system as shown in Fig. 1 (a). The line of length 200 km is modelled using frequency dependant phase model of the PSCAD/EMTDC tool. Voltage and current measurements from both the ends of the line are measured and sampled at 1 kHz. We discuss two cases: (i) when data is synchronized (ii) when data is unsynchronized. In each case, the line loading is varied, and the estimated synchronization angle δ_{est} based on (5) is recorded. The line loading is varied by changing the voltage phase angle between the sources S1 and S2. The actual line loading angle (θ) is calculated as the phase angular difference between voltage phasors at bus M and bus N without any synchronization errors. As $\delta_{est} = \delta + \psi$, the corruption term ψ is computed as the difference of angle between δ and the estimated δ_{est} for the analysis purpose. Results are presented in Table 1.

CASE 1: *Synchronized data*

Synchronized data refers to the case when $\delta = 0^0$. It can be observed from the results of Case 1 that when the load angle is 0^0, the method of [21] works correctly. But as the loading increases, the estimates of the synchronization angle (δ_{est}) deviate from 0^0. This means that the method estimates finite synchronization angles even when there is no synchronization error in the data. Also, the value of ψ closely follows that of θ for light loading, which cannot be seen for higher loading.

CASE 2: *Unsynchronized data*

In this case, the remote end voltage and current measurements are advanced by one sample. In a 50 Hz system, for 1 kHz sampling frequency this data synchronization error translates to a phase angle of 18^0 between the corresponding local and remote end phasors. Similar observations can also be made for this case as well. With increasing loading of the line, the estimated synchronization angle deviates from the actual value of 18^0 and the deviation correlates with the line loading angle only for light loading conditions. Therefore, the method for estimation of the synchronization angle proposed in [21] can lead to incorrect results, which will subsequently affect the steps of line parameter and fault distance estimation. To overcome the limitations thus analyzed, a reliable and improved method is proposed in the next section.

Table 1 Analysis of synchronization angle calculation

Case	δ (°)	$\angle\bar{E}_1 - \angle\bar{E}_2$ (°)	θ (°)	δ_{est} [21] (°)	ψ (°)
Case 1	0	0	0.0349	**-0.0072**	-0.0072
		10	8.1859	7.1409	7.1409
		20	16.3357	21.4974	21.4974
		30	24.5261	-69.6868	-69.6868
		50	41.1965	-10.6524	-10.6524
Case 2	18	0	0.0349	**18.0071**	0.0071
		10	8.1859	25.1424	7.1424
		20	16.3357	39.4910	21.4910
		30	24.5261	-51.7692	-69.7692
		50	41.1965	7.3353	-10.6647

3 Proposed Method

The proposed method eliminates the influence of line loading on the estimated synchronization angle. A mathematical derivation of the important steps and the implementation methodology are described here.

3.1 Correct formulation for synchronization angle estimation

Using $\delta_{est} = \delta + \psi$, (6) can be written as,

$$e^{j2\delta} \cdot e^{j2\psi} = \frac{(\bar{F}_1^*\text{-}\,\bar{F}_2)}{(\bar{F}_1\text{-}\,F_2^*)} \tag{9}$$

From the properties of complex numbers,

$$\tfrac{1}{2}(\cosh\gamma l_{MN} - (\cosh\gamma l_{MN})^*) = \mathrm{j}\,\mu \tag{10}$$

where μ, the imaginary part of $\cosh\gamma l_{MN}$ is considered as a "design factor" in this paper. Its inclusion in the formulation for synchronization angle estimation eliminates influence of line loading. It can be estimated from a set of synchronized measurements and stored. Alternatively, it can be computed from the line design parameters available during commissioning of the line. The factor can be computed irrespective of the loading and can be used at any other loading condition when data is not synchronized. The synchronization angle estimated using the method proposed in this paper is denoted as δ_P. Substituting (3) in (10) we obtain,

$$\mathrm{e}^{j2\delta_P}(\bar{F}_1\text{-}\,\bar{F}_2^*) - j2\mu e^{j\delta_P}\text{-}\,(\bar{F}_1^*\text{-}\,\bar{F}_2) = 0 \tag{11}$$

Equation (11) is quadratic in the variable $e^{j\delta_P}$ which can be solved to obtain two possible roots as below:

$$e^{j\delta_P} = \frac{j2\mu \pm \sqrt{-4\mu^2 + 4(\bar{F}_1 - \bar{F}_2^*)(\bar{F}_1^* - \bar{F}_2)}}{2(\bar{F}_1 - \bar{F}_2^*)} \tag{12}$$

Note in (12), $\bar{F}_1$ and $\bar{F}_2$ are computed by the expressions provided previously in (3) of Section 2 using the unsynchronized voltage and current measurements.

3.2 Selection of valid solution

Two values of δ_P obtained from (12) are used to get two corresponding sets of line parameters (γ and z_c) using (1), (2) and (3) [21].

$$\gamma = \frac{\cosh^{-1}(\bar{F}_1 e^{j\delta_P} + \bar{F}_2 e^{-j\delta_P})}{l_{MN}} \quad (13)$$

$$Z_c = \frac{\bar{V}_M \sinh \gamma l_{MN}}{\bar{I}_N e^{j\delta_P} + \bar{I}_M \cosh \gamma l_{MN}} \quad (14)$$

The valid solution set from the two sets of δ_P, γ and Z_c can be selected by performing the following checks [22].

$$\text{real}(\gamma^2)<0 \text{ and real}(Z_c^2)>0 \quad (15)$$

$$\text{imag}(\gamma^2)>0 \text{ and imag}(Z_c^2)<0 \quad (16)$$

In situations where (15) and (16) are satisfied by both of the solution sets, an additional check shown in (17) need to be performed.

$$\text{R}>0 \text{ and X}>0 \text{ and Y}>0 \quad (17)$$

Here R, X and Y are line resistance, reactance and admittance respectively. They can be obtained from γ and z_c.

3.3 Estimation of fault location

From Fig.1 (c), correct solution set can be further used to estimate the fault location (d) using the below [21]

$$\text{d} = \frac{1}{\gamma l_{MN}} \tanh^{-1}\left[\frac{(\text{A}e^{j\delta_P} + B)}{(Ce^{j\delta_P} + D)}\right] \quad (18)$$

where $\bar{V}_{Mf}, \bar{V}_{Nf}, \bar{I}_{Mf}, \bar{I}_{Nf}$ are positive sequence phasors derived from during-fault unsynchronized measurements and

$A = \bar{I}_{Nf} Z_c \sinh \gamma l_{MN} - \bar{V}_{Nf} \cosh \gamma l_{MN}$; $B = \bar{V}_{Mf}$

$C = \bar{I}_{Nf} Z_c \cosh \gamma l_{MN} - \bar{V}_{Nf} \sinh \gamma l_{MN}$; $D = \bar{I}_{Mf} Z_c$

Flowchart of the proposed method is given in Fig. 2 and the results are discussed in the next section.

4 Experimental Results

The results presented in this section are based on the test system introduced in Section 2.

4.1 Illustration of the Proposed Method

We illustrate the proposed method for the case discussed previously in Section 2 relating to unsynchronized data. Results are presented in Table 2. From the table, it can be seen that unlike the method of [21], the proposed methodology estimates the synchronization angle accurately for all line loading conditions.

Table 2 Determined synchronization angle

$\angle\bar{E}_1 - \angle\bar{E}_2$ (°)	δ_{est}(°)[21]	δ_P(°)
0	18.0071	17.999
10	25.1424	18.005
20	39.4910	18.015
30	-51.7692	17.888
50	7.3353	17.991

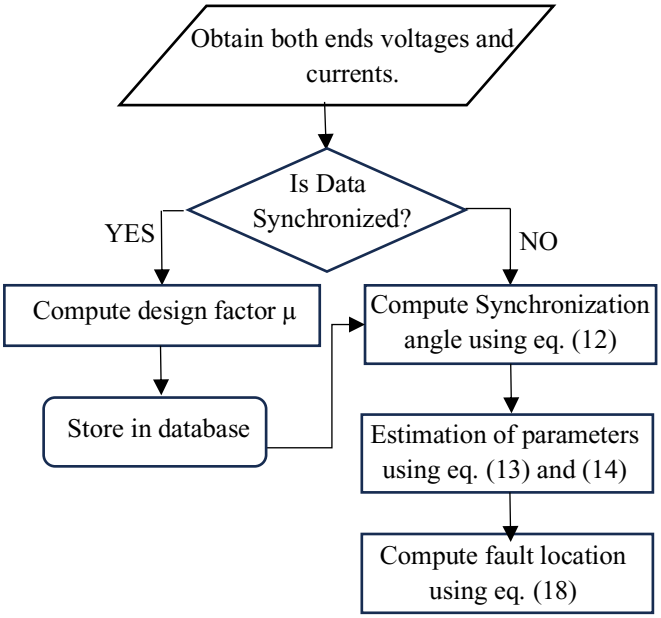

Fig.2. Flow chart of proposed method

4.2 Comparative Analysis

In this section, comparative analysis of the proposed method with [20, 21] for the computation of synchronization angle, line parameters and fault location using synchronized and unsynchronized data is presented. The actual parameters of the line are listed in the Table 3 for comparison purpose.

Table 3 Actual line parameters

	R (Ω/km)	X (Ω/km)	B ($\mu S/km$)
Actual Value	0.0346	0.4233	2.7259

Four cases covering different line loading conditions, fault locations, fault resistance and data synchronizations are simulated to demonstrate the validity of the proposed method and the results are compared with [20, 21].

4.2.1 Synchronized Data: In this section, two cases are presented using synchronized data to compare the proposed method with existing literature [20, 21].

CASE 1- *A-G fault at 40km from Bus M with a fault resistance of 50 Ω, load angle is* 0^0: The data synchronization angle and parameters are estimated by using the proposed method and available methods for this case. The results are listed in Table 4. The proposed and existing methods calculates the line parameters accurately and error is within 1%. As second step, the fault location is calculated using the estimated parameters and during fault phasors and results are presented in Table 5.

Table 4 Estimated synchronization angle and parameters

Method	Estimated δ (°)	R (Ω/km) (%)	X (Ω/km) (%)	B ($\mu S/km$) (%)
[20]	NA	0.0350 (1.15)	0.4203 (0.71)	2.7393 (0.49)
[21]	0.014	0.0351 (1.45)	0.4293 (1.42)	2.7278 (0.07)
Proposed	0	0.0350 (1.15)	0.4205 (0.66)	2.7296 (0.14)

Table 5 Calculated fault location for Case 1

Method	Estimated fault location (km)	Error (km)	Error (%)
[20]	39.237	0.763	0.38
[21]	40.911	0.911	0.46
Proposed	39.337	0.663	0.33

The proposed and existing methods [20, 21] locate the fault within two tower span distance for this case.

CASE 2- *AB fault at 75km from Bus M with a fault resistance of 10 Ω, load angle is* 20^0: The estimated synchronization angle, parameters and fault location results are provided in Table 6 and 7 respectively. Synchronization angle and line parameters estimated using the method in [21] are not accurate as it depends on the loading conditions, whereas the proposed method calculated the synchronization angle and parameters correctly for this case. The proposed method and method in [20] located the fault accurately whereas the method presented in [21] failed to locate the fault accurately.

Table 6 Estimated synchronization angle and parameters

Method	Estimated δ (°)	R (Ω/km) (%)	X (Ω/km) (%)	B $(\mu S/km)$ (%)
[20]	NA	0.0343 (0.87)	0.4202 (0.73)	2.7423 (0.60)
[21]	21.642	0.5886 (1601.20)	2.8839 (581.29)	74.867 (2646.50)
Proposed	0.009	0.0346 (0)	0.4237 (0.09)	2.7345 (0.32)

Table 7 Calculated fault location for Case 2

Method	Estimated fault location (km)	Error (km)	Error (%)
[20]	75.203	0.203	0.10
[21]	105.892	30.892	15.45
Proposed	75.125	0.125	0.06

4.2.2 Unsynchronized Data: In this section, two cases are presented using unsynchronized data to compare the proposed method with existing literature [20, 21].

CASE 1*- BC-G fault at 100km from Bus M with a fault resistance of 20 Ω, load angle is* 0^0: A data synchronization error of 36^0 is considered in this case. The results for synchronization angle and line parameters are presented in Table 8 whereas fault location results are presented in Table 9. The synchronization angle obtained with both the methods is close to the actual value. The fault location estimated using both the methods is giving good accuracy which is a difference of 121m and 111m respectively for this loading condition. The method proposed in [20] is not designed for unsynchronized data and it will not work for this case.

Table 8 Estimated synchronization angle and parameters

Method	Estimated δ (°)	R (Ω/km) (%)	X (Ω/km) (%)	B $(\mu S/km)$ (%)
[21]	36.007	0.0351 (1.45)	0.4575 (8.08)	2.7288 (0.11)
Proposed	35.999	0.0348 (0.58)	0.4264 (0.73)	2.7297 (0.14)

Table 9 Calculated fault location for the Case 1

Method	Estimated fault location (km)	Error (km)	Error (%)
[21]	99.879	0.121	0.06
Proposed	100.111	0.111	0.05

CASE 2*- ABC-G fault at 175km from Bus M with a fault resistance of 0.01 Ω, load angle is* 10^0: The data synchronization error of 54^0 is considered in this case where remote end data is advanced by 3 samples. The results for the synchronization angle calculation and parameters are presented in Table 10. Proposed method outperforms and obtains accurate results for synchronization angle, line parameters as well as fault location. Whereas [21] provides erroneous result due to the effect of loading on the method. The fault location estimated using [21] gives ~70km error which is undesirable whereas proposed method gives an error of only 171m which is equivalent to ~1-2 tower span as presented in Table 11.

Table 10 Estimated synchronization angle and parameters

Method	Estimated δ (°)	R (Ω/km) (%)	X (Ω/km) (%)	B $(\mu S/km)$ (%)
[21]	61.15	0.2349 (578.9)	-0.0028 (NA)	-3.5122 (NA)
Proposed	54.003	0.0348 (0.58)	0.4231 (0.05)	2.7267 (0.03)

Table 11 Calculated fault location for the Case 2

Method	Estimated fault location (km)	Error (km)	Error (%)
[21]	244.223	69.223	34.61
Proposed	175.171	0.171	0.09

We can conclude from the above results that the proposed method can estimate the data synchronization angle and parameters using the pre-fault data for all loading conditions. The method can locate fault within 2 tower span distance which can be very advantageous for the utilities in fault management. The method is further validated with field data and results are provided in the next section.

5 Validation with Field Data

The proposed method is validated with two transmission lines located in Sweden and India [20].

System 1: A 220-kV, 265.6 km transmission line connected between Station A and Station B.
System 2: A 400-kV, 233.07 km transmission line connected between Station A and Station B.

Field Case 1*- Fault at 226.6 km for System 1 from Station A:* Double phase fault occurred in System 1 on 14th July 2021. The estimated synchronization angle and line parameters are provided in Table 12 and fault location results are listed in Table 13. Calculated fault location using the proposed method, method [20] and [21] are 226.439km, 226.82km and 5.16km from station A respectively. When the line crew patrolled the line, they found a fault at 226.6 km from station A. The proposed method matches the actual value.

Table 12 Estimated synchronization angle and line parameters

Method	Synchronization angle (°)	R (Ω)	X (Ω)	B (mS)
[20]	NA	14.166	84.85	1000.548
[21]	16.8200	33.332	823.362	11974
Proposed	0	15.388	85.866	995.1

Table 13 Calculated fault location for the Field Case 1

Actual fault location(km)	Method	Estimated fault location (km)	Error (km)	Error (%)
226.6	[20]	226.82	0.22	0.08
	[21]	5.163	221.44	83.37
	Proposed	226.439	0.439	0.06

The difference of actual to estimated fault location is within ± 1 tower span when using the proposed method and method of reference [20] for this case whereas the method [21] located the fault at 5.16 km, thus giving severely erroneous estimate even when the data is perfectly synchronized.

Field Case 2*- Fault at 33 km for System 2 from Station A:* Phase C to ground fault occurred in System 2 on 21 September 2021. The estimated synchronization angle and line parameters are provided in Table 14 and fault location results are listed in Table 15. Calculated fault location using the proposed method, method [20] and [21] are 32.93km, 32.87km, and 104.92km from station A respectively. The proposed method matches the actual fault location identified by the line patrolling crew.

Table 14 Estimated synchronization angle and line parameters

Method	Synchronization angle (°)	R (Ω)	X (Ω)	B (mS)
[20]	NA	5.269	68.830	901.105
[21]	-172.6511	207.9742	3.1268	673.9
Proposed	-2.63e-15	5.112	69.298	897.7

Table 15 Calculated fault location for the Field Case 2

Actual fault location(km)	Method	Estimated fault location (km)	Error (km)	Error (%)
33	[20]	32.87	0.13	0.06
	[21]	104.921	71.921	30.86
	Proposed	32.934	0.066	0.03

Field Case 3*- Fault at 114.47 km for System 2 from Station A:* Phase B to ground fault occurred on 24 April 2022. The data is unsynchronized at the time of the fault. The method [20] is not applicable for this case. The estimated synchronization angle and line parameters using the proposed method and the method of [21] are provided in Table 16. Fault location results are listed in Table 17.

Table 16 Estimated synchronization angle and line parameters

Method	Synchronization angle (°)	R (Ω)	X (Ω)	B (mS)
[21]	112.5071	18.009	28.468	749.6
Proposed	**72.04**	5.413	69.738	897.6

Table 17 Calculated fault location for the Field Case 3

Actual fault location(km)	Method	Estimated fault location (km)	Error (km)	Error (%)
114.47	[21]	122.881	8.411	3.61
	Proposed	115.119	0.649	0.28

Calculated fault location using the proposed method and [21] are 115.11km and 122.88km from station A respectively. The proposed method matches the actual fault location identified by the line patrolling screw. Validation with field data proved that the proposed method has located the fault accurately with both synchronized and unsynchronized data. The performance of the method is superior to the existing synchronized data [20] and unsynchronized data [21] methods.

5 Conclusions

A setting-free method for fault location on transmission lines using unsynchronized terminal measurements is proposed. The method is based on an accurate estimation of the data synchronization angle. This is done using a design factor which avoids corruption of the angle estimation due to line loading. The factor is calculated and stored in the database using a previously available set of synchronized data at any load condition. The advantage of the proposed method over existing methods is illustrated using a 400kV, 200 km transmission line. It is observed that unlike the existing solutions, the method proposed can accurately estimate the synchronization angle without getting influenced by the line loading. This in turn results in accurate line parameter and eventually fault location estimates (within ± 1 tower span), while the existing methods suffer from (a) being limited in application to perfectly synchronized data or (b) estimating the synchronization angle inaccurately when data is not perfectly synchronized. The results from numerical experiments are validated using field records of actual fault events with both synchronized and unsynchronized measurements. The proposed method clearly outperforms the existing solutions.

6 References

[1] M. M. Saha, J. Izykowski and E. Rosolowski, Fault Location on Power Networks, London, U.K.:Springer, 2010.

[2] "IEEE Guide for Determining Fault Location on AC Transmission and Distribution Lines," in IEEE Std C37.114-2014 (Revision of IEEE Std C37.114-2004), vol., no., pp.1-76, Jan. 2015.

[3] T. Takagi, Y. Yamakoshi, M. Yamaura, R. Kondow and T. Matsushima, "Development of a New Type Fault Locator Using the One-Terminal Voltage and Current Data," in *IEEE Transactions on Power Apparatus and Systems*, vol. PAS-101, no. 8, pp. 2892-2898, Aug. 1982.

[4] L. Eriksson, M. M. Saha and G. D. Rockefeller, "An Accurate Fault Locator With Compensation For Apparent Reactance In The Fault Resistance Resulting From Remote-End Infeed," in *IEEE Transactions on Power Apparatus and Systems*, vol. PAS-104, no. 2, pp. 423-436, Feb. 1985.

[5] S. Das, S. Santoso, A. Gaikwad and M. Patel, "Impedance-based fault location in transmission networks: theory and application," in *IEEE Access*, vol. 2, pp. 537-557, 2014.

[6] Neethu George and O. D. Naidu, "Distance Protection Issues with Renewable Power Generators and Possible

Solutions," *16th International Conference on Developments in Power System Protection (DPSP 2022),* Mar.2022, pp. 1-6.
[7] L. Kukkala, O. D. Naidu, A. V and S. Sharma, "Single Ended Fault Locator for Power Transmission Lines Connected with Inverter Based Resources: Problems and Mitigation Approach," *2022 22nd National Power Systems Conference (NPSC),* New Delhi, India, 2022, pp. 685-690.
[8] V. Pradhan, N. George, O. Naidu, Z. Gajic and S. Zubic, "Distance protection of inverter-based renewables power evacuating lines and downstream network: Issues and mitigation approach," *2022 IEEE PES Innovative Smart Grid Technologies - Asia (ISGT Asia),* Singapore, Singapore, 2022, pp. 215-219.
[9] E. O. Schweitzer, A. Guzman, M. V. Mynam, V. Skendzic, B. Kasztenny, and S. Marx, "Locating faults by the traveling waves they launch," in *Proc.67th Annu. Conf. Protective Relay Eng.,* Nov. 2014, pp. 95–110.
[10] O. D. Naidu and A. K. Pradhan, "Precise Traveling Wave-Based Transmission Line Fault Location Method Using Single-Ended Data," in *IEEE Transactions on Industrial Informatics*, vol. 17, no. 8, pp. 5197-5207, Aug. 2021.
[11] O. D. Naidu and A. K. Pradhan, "Model Free Traveling Wave Based Fault Location Method for Series Compensated Transmission Line," in *IEEE Access*, vol. 8, pp. 193128-193137, Oct.2020.
[12] O. D. Naidu and A. K. Pradhan, "A Traveling Wave-Based Fault Location Method Using Unsynchronized Current Measurements," in *IEEE Transactions on Power Delivery*, vol. 34, no. 2, pp. 505-513, April 2019.
[13] T. -C. Lin, J. -Z. Yang, C. -S. Yu and C. -W. Liu, "Development of a Transmission Network Fault Location Platform Based on Cloud Computing and Synchrophasors," in *IEEE Transactions on Power Delivery*, vol. 35, no. 1, pp. 84-94, Feb. 2020.
[14] D. A. Tziouvaras, J. B. Roberts and G. Benmouyal, "New multi-ended fault location design for two- or three-terminal lines," *2001 Seventh International Conference on Developments in Power System Protection (IEE*), 2001, pp. 395-398.
[15] J. Izykowski, R. Molag, E. Rosolowski and M. M. Saha, "Accurate location of faults on power transmission lines with use of two-end unsynchronized measurements," in *IEEE Transactions on Power Delivery*, vol. 21, no. 2, pp. 627-633, April 2006.
[16] D. Novosel, D. G. Hart, E. Udren and J. Garitty, "Unsynchronized two-terminal fault location estimation," in *IEEE Transactions on Power Delivery*, vol. 11, no. 1, pp. 130-138, Jan. 1996.
[17] J. Izykowski, E. Rosolowski, P. Balcerek, M. Fulczyk and M. M. Saha, "Accurate Noniterative Fault Location Algorithm Utilizing Two-End Unsynchronized Measurements," in *IEEE Transactions on Power Delivery*, vol. 25, no. 1, pp. 72-80, Jan. 2010.
[18] O.D. Naidu, P. Yalla, A. V.S.S.R. Sai and S. Sawai, "Model-free fault location for transmission lines using Phasor Measurement Unit data." in *CIGRE Study Committee B5 Colloquium*, vol. 5, pp. 1-12, Jun 2019.
[19] K. J. Kusic and D. L. Garrison, "Measurement of transmission line parameters from SCADA data", *IEEE PES Power System Conference and Exposition*, New York, USA, Oct. 2004.
[20] O. D. Naidu, S. Zubic, A. V. S. S. R. Sai, A. N. Praveen, P. Cost and H. Eriksson, "Economical Setting-Free Double-Ended Fault Locator for Transmission Lines: Experiences From Recent Pilot Installations," in *IEEE Access*, vol. 10, pp. 96805-96820, 2022.
[21] K. Kalita, S. Anand and S. K. Parida, "A Closed Form Solution for Line Parameter-Less Fault Location With Unsynchronized Measurements," in *IEEE Transactions on Power Delivery*, vol. 37, no. 3, pp. 1997-2006, June 2022.
[22] O. D. Naidu, N. George and P. Yalla, "Setting-free Fault Section Identification and Fault Location Method for Three-terminal Lines," *2019 9th International Conference on Power and Energy Systems (ICPES),* Perth, WA, Australia, 2019, pp. 1-6, doi: 10.1109/ICPES47639.2019.9105476.